

Effect-Level Validation for Causal Discovery

Hoang Dang
Independent Researcher
Vietnam
hoangdang112023@gmail.com

Luan Pham
RMIT University
Australia
luan.pham@rmit.edu.au

Minh Nguyen
Florida Atlantic University
USA
minhnguyen@fau.edu

Abstract

Causal discovery is increasingly applied to large-scale telemetry data to estimate the effects of user-facing interventions, yet its reliability for decision-making in feedback-driven systems with strong self-selection remains unclear. In this paper, we propose an effect-centric, admissibility-first framework that treats discovered graphs as structural hypotheses and evaluates them by identifiability, stability, and falsification rather than by graph recovery accuracy alone. Empirically, we study the effect of early exposure to competitive gameplay on short-term retention using real-world game telemetry. We find that many statistically plausible discovery outputs do not admit point-identified causal queries once minimal temporal and semantic constraints are enforced, highlighting identifiability as a critical bottleneck for decision support. When identification is possible, several algorithm families converge to similar, decision-consistent effect estimates despite producing substantially different graph structures, including cases where the direct treatment–outcome edge is absent and the effect is preserved through indirect causal pathways. These converging estimates survive placebo, subsampling, and sensitivity refutation. In contrast, other methods exhibit sporadic admissibility and threshold-sensitive or attenuated effects due to endpoint ambiguity. These results suggest that graph-level metrics alone are inadequate proxies for causal reliability for a given target query. Therefore, trustworthy causal conclusions in telemetry-driven systems require prioritizing admissibility and effect-level validation over causal structural recovery alone.

CCS Concepts

• **Computing methodologies** → **Causal reasoning and diagnostics**; • **Information systems** → **Data mining**.

Keywords

causal discovery, causal inference, game telemetry, effect validation

1 Introduction

Large-scale telemetry data from online platforms and interactive systems have made causal discovery an attractive tool for understanding user behavior and guiding product decisions [3, 13–15, 19]. Yet these systems are characterized by feedback loops, strong self-selection into features, and composite metrics that conflate causes with consequences—properties largely absent from the synthetic benchmarks on which discovery methods are typically evaluated. While recent advances aim to reconstruct causal graphs from observational data, practitioners ultimately require reliable answers to concrete causal inference questions, such as whether feature

X *causally* increases user retention, rather than knowing a single “correct” structural causal graph [3, 13–15, 19].

Most prior work [5, 20, 21] evaluates causal discovery using graph-level recovery metrics (e.g., SHD, precision, recall) against synthetic ground truth, implicitly assuming that structural accuracy implies causal reliability. However, this assumption breaks down in real-world telemetry systems with feedback loops and strong self-selection. Multiple causal graph structures can be statistically compatible with the observational data, yet only a subset admit valid identification strategies for a target causal query once minimal temporal and semantic constraints are enforced.

In this study, our central research question is: **How should a causal effect derived from discovered structures be trusted for decision-making in feedback-driven telemetry systems?**

We argue that this is an effect-level decision problem rather than a graph recovery problem. The objective is not to select a single best graph but to determine whether a target causal estimand remains identifiable, stable, and robust to falsification under structural uncertainty. We propose an effect-centric, admissibility-first framework that treats discovered structures as structural hypotheses and filters them by identifiability and overlap (positivity) before effect estimation. Reliability is assessed through effect stability across algorithms and significance thresholds, placebo and subsampling refutation tests, and sensitivity analysis to unmeasured confounding.

We instantiate this framework on real-world game telemetry data to study the effect of early competitive gameplay (PvP) on short-term retention [13]. The dataset comprises behavioral telemetry from a deployed role-playing game, where paying players who voluntarily enter competitive modes differ sharply from non-participants across engagement, progression, and platform commitment. Our results reveal a disconnect between graph-level plausibility and effect-level reliability. Several statistically plausible structures produced by latent-aware discovery methods do not yield identifiable estimands under the enforced domain constraints. In contrast, a subset of algorithms (PC, GRASP, BOSS) converge to a common effect magnitude that matches the domain-admissible causal effect, despite producing structurally different graphs and, in some cases, lacking a direct treatment–outcome edge.

Our findings challenge the established practice of evaluating causal discovery by using structural accuracy alone. Graphs with favorable structural scores can fail to identify the target estimand, while structurally divergent graphs can yield identical, validated effects, decoupling graph-level fit from causal reliability. They show that in feedback-driven systems, identifiability and effect stability, not graph recovery, are the primary bottlenecks. We conclude that causal discovery should be assessed by whether it supports trustworthy causal answers rather than by how closely it approximates an unknown ground-truth graph. In practice, this means discovery pipelines should incorporate admissibility gates, stability checks,

and falsification tests as standard evaluation criteria alongside, or in place of, graph recovery metrics.

In summary, our key contributions are:

- (1) **Admissibility-first, effect-centric framework.** We propose a pipeline that treats discovered graphs as structural hypotheses and filters them by causal admissibility (identifiability and positivity) before effect estimation, shifting evaluation from graph recovery to query reliability under structural uncertainty.
- (2) **Effect-level validation protocol.** We introduce a validation protocol combining overlap diagnostics, refutation tests (placebo and subsampling), and sensitivity analysis (E-values) to assess when a discovered causal effect can be trusted.
- (3) **Empirical evidence of effect convergence under domain constraints.** Using real-world game telemetry, we show that several causal discovery algorithm families converge to similar, decision-consistent effect estimates despite producing structurally divergent graphs, including cases where the effect operates entirely through indirect causal pathways.
- (4) **Characterization of identifiability bottlenecks.** We show that only a subset of causal discovery outputs admit point-identified causal queries once minimal temporal and semantic constraints are enforced, and characterize how unresolved orientations and structural ambiguity prevent identification. Therefore, identifiability and effect stability cannot be inferred from algorithm families or graph-level metrics alone.

Our replication package, including code and data, is available at <https://anonymous.4open.science/r/kdd26-causal/>.

2 Related Work

Causal Inference in Interactive Platforms. Causal inference has been increasingly adopted in large-scale online platforms such as recommender systems [9], e-commerce marketplaces [29], and social media services, where randomized experimentation is costly, incomplete, or infeasible. [28] document how confounding, missing-not-at-random exposure, and feedback loops invalidate purely predictive approaches in these systems. These works emphasize that user behavior is shaped by platform policies themselves, making observational data inherently biased. Recent studies demonstrate that causal modeling is essential for evaluating engagement-oriented outcomes, such as retention or long-term usage, which cannot be reliably optimized using short-term predictive metrics [3, 15]. However, most existing work in this space assumes known causal structure, either specified by domain experts or derived from experiments, rather than addressing how discovery-induced structural uncertainty propagates to effect estimates [7]. Our work confronts this gap by evaluating whether effects derived from discovered structures remain reliable under structural ambiguity.

System-Centric Causal Analysis. Causal inference has also been applied to system-diagnosis problems, most notably root cause analysis in microservices. [11, 20] demonstrate how causal graphs learned from high-dimensional telemetry can localize root causes without requiring full system observability. These studies emphasize scalability, robustness, and the ability to operate under partial intervention data as central design constraints. While online games involve human agency unlike purely automated microservices, both domains share a telemetry-driven architecture where

latent system states and causal dependencies must be inferred from high-dimensional, noisy metric streams under partial observability. Our setting differs in that the target query is an average treatment effect on a user-level outcome rather than a localization or ranking task, placing additional demands on identifiability and effect-level validation that system-diagnosis frameworks do not address.

Causal Inference in Video Game Telemetry. In video game telemetry, causal inference is complicated by strong feedback loops and simultaneity between player behavior and system state. [6] show that standard predictive or correlational analyses of in-game performance metrics are systematically biased, as these metrics are both causes and consequences of match outcomes. By leveraging randomized hero assignments as instrumental variables, the study demonstrates that correlation-based models substantially misestimate causal effects in competitive games. [17] provide a serial mediation framework for decomposing long-term outcomes, modeling retention as the cumulative effect of sequential mediators rather than a direct response to a single action. Broader game analytics research has examined how matchmaking quality [13], achievement systems [19], and progression design [14] influence retention, but these studies rely on pre-specified causal structures or correlational analyses rather than discovery-based approaches. Collectively, these works establish that correlation is insufficient for identifying causal mechanisms in games, but none addresses how structural uncertainty from causal discovery propagates to downstream effect estimates, the gap our framework targets.

Validation Without Ground Truth. Evaluating causal models in real-world systems remains challenging due to the absence of ground-truth structural causal graphs. Recent studies [10, 20] argue that edge-level accuracy on synthetic benchmarks is a poor proxy for real-world utility, advocating instead for evaluation based on interventional performance. [8] proposes refutation-style validation based on variable-subset stability, offering a complementary approach that does not require interventional data. These approaches align with a growing consensus that causal validation must rely on robustness, stability, and downstream intervention performance rather than structural recovery alone. Our work follows this philosophy by validating through effect-level criteria, including identifiability gates, stability across algorithms and thresholds, placebo and subsampling refutation, and sensitivity analysis for unmeasured confounding, applied systematically across multiple discovery outputs rather than to a single pre-specified graph.

3 Methodology

3.1 Overview

We study a decision problem rather than a graph recovery problem. Given observational telemetry from an interactive system characterized by feedback and self-selection, our central question is: **How should a causal effect estimate derived from discovered structures be trusted?**

The inputs to our analysis are: (i) temporally aggregated observational telemetry, (ii) a target causal query specified by a treatment-outcome pair and estimand, and (iii) a set of minimal domain constraints encoding temporal and semantic invariants. The output is: (i) an estimated causal effect with uncertainty when identification

is possible, and (ii) a decision assessment (trust, caution, or reject) based on admissibility, stability, and falsification diagnostics.

We treat causal discovery as a generator of structural hypotheses rather than a definitive estimator. Multiple graphs may be statistically admissible under conditional independence testing, yet many of them fail to support valid causal identification once domain constraints and positivity requirements are enforced, under our DAG-only admissibility gate. In such cases, the target causal query is undefined and no effect can be estimated.

We focus on constraint-based and latent-aware discovery methods that scale to telemetry settings and accommodate mixed discrete-continuous variables. Discovery is performed on temporally sliced variables, assuming acyclicity within each slice. This reflects the operational context of telemetry analysis: although the system evolves through long-term feedback, the causal queries of interest (e.g., early exposure \rightarrow short-term retention) are defined within explicitly ordered time windows.

Domain knowledge is incorporated through a set of minimal temporal and semantic constraints specifying forbidden and required edge directions. These constraints encode invariants such as temporal precedence (future outcomes cannot cause past behaviors) and semantic coherence (platform-level attributes are not caused by downstream gameplay events). They are not intended to enforce the existence of a specific causal pathway between the treatment and outcome, but to exclude causally meaningless configurations.

Accordingly, we introduce an admissibility-first pipeline. Discovered structures are first filtered by whether they admit a valid identification strategy for the target estimand and satisfy positivity requirements. Effect estimation is performed only on graphs that pass this admissibility gate, and stability and falsification are evaluated on this restricted set. Identification failure (yielding undefined effects) is therefore an expected and informative outcome of the pipeline rather than an error condition.

We evaluate constraint-based methods (PC, FCI, FCI-MAX), score-based methods (BOSS, GRaSP), and hybrid approaches (GFCI, BOSS-FCI, GRaSP-FCI). Algorithmic details are provided in Appendix A.

3.2 Graph-Level Baseline Comparison

Before turning to effect-level analysis, we summarize the structural outputs produced by different discovery algorithms. For real-world game telemetry, no ground-truth causal graph is available; therefore, standard graph recovery metrics such as structural Hamming distance (SHD), precision, and recall cannot be interpreted as measures of correctness in the usual benchmark sense.

We report graph-level deviations relative to one domain-admissible baseline structure obtained using pre-specified temporal and semantic constraints. This baseline is not treated as ground truth, but as a reference point for describing how much different algorithms diverge from a constraint-consistent hypothesis.

Table 4 shows that different algorithms produce structurally diverse hypotheses even under the same constraints. Some methods achieve low SHD or high F1 relative to the baseline, while others diverge substantially. However, these differences are not predictive of whether a discovered structure supports a valid causal estimand.

In subsequent sections, we show that several graphs with favorable graph-level metrics fail the admissibility gate and do not admit

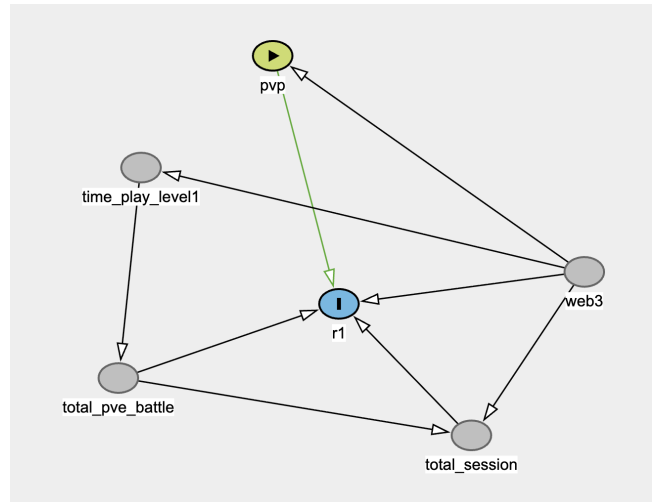


Figure 1: Domain-admissible causal graph constructed with pre-specified constraints. This graph satisfies temporal and semantic invariants and admits valid backdoor identification for the target estimand.

identifiable causal effects for the target query. Conversely, graphs with less favorable structural similarity may still yield admissible and stable effect estimates. This decoupling underscores a central point of the paper: in feedback-driven telemetry systems, structural proximity to a reference graph is neither necessary nor sufficient for effect-level validity.

Accordingly, we treat graph-level comparisons as descriptive context rather than evaluative criteria. All substantive conclusions in this work are based on effect-level diagnostics, identifiability, stability, and falsification, rather than graph recovery scores.

Across all evaluated algorithms, adjacency recall is similar for most algorithms, though some methods show higher recall and lower precision. In contrast, orientation recovery exhibits substantial variability, resulting in non-trivial differences in SHD despite similar skeletons. This highlights that, under strong domain constraints, structural disagreement is dominated by edge orientation rather than edge existence.

3.3 Domain-Admissible Graph

We construct a domain-admissible baseline causal graph entirely from domain knowledge and prior literature on gameplay mechanics and telemetry semantics (Figure 1). All edges are specified a priori using temporal ordering and variable definitions, without data-driven structure learning.

The graph encodes two invariants: (i) temporal constraints that prevent future outcomes from causing earlier behaviors, and (ii) semantic constraints reflecting how telemetry variables are constructed and aggregated (e.g., session counts as components of engagement rather than independent causes).

This structure is effect-agnostic: it does not encode conclusions about the $PvP \rightarrow$ retention, but restricts the hypothesis space to causally interpretable models given the telemetry schema. It is not asserted as ground truth, but serves as one admissible structural

hypothesis that defines a concrete estimand when identification is possible and provides a reference for effect-level comparison across alternative discovered graphs.

As shown in Section 5, many statistically plausible structures fail to admit valid adjustment once minimal temporal and semantic constraints are enforced, motivating our admissibility-first filtering before effect estimation. The full constraint specification is provided in Appendix B.

3.4 Identification and Admissibility

Causal effect estimation in this work is conditional on identifiability. We treat identification not as a modeling preference, but as a hard admissibility criterion: a discovered structure either supports causal estimation for the target query or it does not.

The target estimand is the average treatment effect (ATE) of early competitive exposure on short-term retention. Identification relies on standard adjustment-based criteria. Specifically, a graph is considered admissible for effect estimation if and only if it admits a valid adjustment set that blocks all backdoor paths from treatment to outcome and contains no descendants of the treatment.

Formally, let T denote early PvP exposure and Y denote Day-1 retention. A graph G is admissible if there exists a set W such that: (1) W blocks all backdoor paths from T to Y in G , and (2) W contains no descendants of T .

Graphs that fail to satisfy these conditions are excluded from downstream analysis, regardless of their statistical fit or discovery scores. This is a critical distinction from conventional discovery evaluation: a graph may achieve low SHD and high precision yet still be causally unusable if constraint enforcement disrupts the required adjustment structure.

In telemetry systems with feedback and composite variables, enforcing domain constraints can alter edge orientations or remove arrowheads, potentially leaving unresolved adjacencies. Such structures may satisfy conditional independence tests yet fail to support any valid adjustment set. In these cases, causal effects are undefined, and estimation appropriately returns missing values rather than numerical artifacts. We interpret this outcome as an identification failure, not as a defect of the estimation procedure.

Beyond graphical criteria, identification also requires the positivity (overlap) assumption. For each admissible adjustment set, we assess whether treated and control units co-occur with non-zero probability across covariate strata. We operationalize this through propensity score diagnostics: estimating treatment probabilities conditional on observed covariates, examining the distribution overlap between treatment groups, and trimming observations that fall outside the common support region. Graphs that admit valid adjustment sets but violate overlap after trimming are flagged as inadmissible for effect estimation under the specified estimand.

By elevating identification and overlap to first-class admissibility gates, we ensure that subsequent comparisons across discovery algorithms evaluate causal reliability, not merely statistical compatibility. This gatekeeping step is essential for distinguishing between graphs that are structurally plausible and those that can support meaningful causal inference in feedback-driven telemetry data.

Some discovery methods return partial ancestral graphs (PAGs) [12] with unresolved edge orientations. To handle this structural

uncertainty, we rely explicitly on PAG-calculus-based admissibility and identification checks, rather than DAG-specific criteria. In particular, we apply PAG-calculus rules to determine whether the target causal query is identifiable under the constraints encoded by the PAG, and we estimate effects only for runs where the calculus certifies a valid adjustment strategy. Consequently, all reported PAG results correspond to point-identified causal effects under PAG-calculus within our framework.

PAG-based estimates are reported separately from the main DAG-based analysis to distinguish identification under partial orientation from fully directed structures. All primary comparisons, stability analyses, and conclusions in the main text are based on DAG-returning methods, while PAG results are provided for complementary reference in Appendix F. Confidence intervals are computed conditional on identification but omitted here for brevity.

3.5 Estimation and Validation

We use DoWhy [4, 25] for causal effect estimation, conditional on passing the admissibility gate. Effect estimation is performed only for graph realizations that (i) admit a valid identification strategy and (ii) satisfy overlap requirements. Discovered structures that fail these criteria are excluded from estimation and reported as identification failures.

For admissible graphs, effects are identified via backdoor or general adjustment and estimated primarily using a doubly robust estimator. This choice provides protection against misspecification of either the outcome or treatment model and aligns with our goal of effect-level reliability under structural uncertainty. For robustness, we also report regression adjustment and IPW estimates as secondary references. Across estimators, results are consistent in sign and magnitude. All reported effects are expressed on the outcome probability scale (risk difference or risk ratio), rather than log-odds, to maintain interpretability for decision support. When common-support trimming is applied to enforce positivity, the resulting estimand should be interpreted as the average treatment effect over the overlap-satisfying subpopulation.

Rather than validating models by graph recovery accuracy, we evaluate estimated effects using complementary effect-level diagnostics aligned with the proposed workflow.

For refutation tests, we apply targeted falsification tests to probe distinct failure modes. A placebo treatment test replaces the true treatment with a randomly permuted variable; a non-null placebo effect would indicate residual confounding or model misspecification. A data subset test re-estimates effects on random subsamples; sensitivity to subsampling suggests overfitting or sample-specific artifacts.

Sensitivity analysis to unmeasured confounding. To assess robustness to unobserved confounders, we compute E-values [27] on the risk-ratio scale. This analysis quantifies the minimum strength of association an unmeasured confounder would need with both treatment and outcome to explain away the observed effect. We treat sensitivity analysis as an additional falsification gate complementing placebo and subsampling tests.

For plausibility checks, we cross-check estimated effects against game design mechanics and domain knowledge. Effects that contradict known operational constraints or design intent warrant additional scrutiny, even if they satisfy statistical diagnostics.

4 Data

4.1 Dataset Overview

We use behavioral telemetry from a deployed Web3 role-playing game (RPG) collected over a 5-month period, comprising 77,698 unique users represented by 26 telemetry-derived features. Data was captured via Firebase telemetry, covering a broad range of in-game activities including gameplay sessions, progression milestones, economic transactions, and system interactions.

This study specifically targets the paying users, yielding an analytic sample of $n = 1,376$ paying players (after quality filters / missingness removal, the analytic sample is $n=1,280$; overlap trimming further yields $n=1,170$)

The unit of analysis is the individual user. For each user, we define the treatment time as the timestamp of their first PvP exposure. All covariates are constructed using only events occurring strictly before this time, ensuring that no post-treatment information is used for discovery, adjustment, or overlap diagnostics.

To ensure strict temporal precedence required for causal inference, data is structured into two non-overlapping time windows:

- Covariate window (t_{0-24h}): All behavioral features and potential confounders are aggregated from the user's first 24 hours of gameplay. No post-treatment information is included.
- Outcome window (t_{24-48h}): The retention outcome is observed in the subsequent 24-hour window (Day 1).

We restrict the analysis to users who remain active up to a fixed PvP eligibility time t_0 . Treatment is defined as engaging in PvP within $[t_0, t_0 + \Delta]$, and all covariates are computed using data prior to t_0 . Users who churn before t_0 are excluded from both groups.

While temporal ordering alone does not eliminate unobserved confounding, this separation ensures that all observed behavioral signals strictly precede the retention outcome, thereby mitigating the risk of reverse causality within the analyzed time slice.

4.2 Variable Definitions

Our causal analysis focuses on six variables selected to isolate the effect of early competitive engagement (PvP mode). A critical design assumption is that participation in the Arena (PvP) mode is an optional gameplay branch, distinct from the mandatory PvE (Player vs. Environment) progression path. This allows us to treat early Arena engagement as a discretionary action (treatment) rather than a forced progression step.

Table 1 provides formal definitions. The treatment variable (PvP) captures voluntary exposure to competitive gameplay loops during the critical first-day window. Covariates include Web3 wallet connection (a proxy for platform commitment and economic investment intent), onboarding intensity (time spent on initial level), baseline PvE activity (progression through non-competitive content), and overall session frequency.

Table 1: Variable Definitions

Variable	Type	Definition
R1 (Outcome)	Binary	Day-1 retention: 1 if user returned during hours 24–48, 0 otherwise
PvP (Treatment)	Binary	Early PvP exposure: participation in competitive mode during first 24 hours
Web3	Binary	Wallet connection status (proxy for platform commitment)
Time_Play_Level1	Continuous	Time spent on Level 1 (onboarding friction proxy)
Total_PvE_Battle	Integer	Number of PvE battles (baseline progression)
Total_Session	Integer	Total login sessions (engagement intensity)

Table 2: Descriptive Statistics by Treatment Status

Variable	Overall	PvP=1	PvP=0
R1 (Retention)	0.71	0.89	0.65
Web3 (Wallet)	0.48	0.73	0.42
Time_Play_Level1	7.83	8.07	7.77
Total_PvE_Battle	10.76	18.87	8.67
Total_Session	3.87	5.32	3.50

4.3 Descriptive Statistics and Self-Selection Evidence

Within this paying-player cohort, 25.86% voluntarily engaged with the PvP mode ($T = 1$) within the first day, while 74.14% relied solely on PvE content ($T = 0$). The overall Day-1 retention rate (R1) is 70.39%.

Table 2 contrasts the engagement profiles of treated and control groups. The differences are striking: PvP-exposed users show 89% retention versus 65% for non-exposed users, a raw difference of 24 percentage points. However, this naive comparison is confounded by severe self-selection: PvP participants are substantially more likely to have connected Web3 wallets (73% vs. 42%), complete more PvE battles (18.87 vs. 8.67), and log more sessions (5.32 vs. 3.50).

These imbalances highlight the core identification challenge: players who voluntarily enter competitive modes are systematically different from those who do not, along dimensions that independently predict retention. The naive treatment-control difference (0.24) therefore conflates the causal effect of PvP exposure with selection effects from unobserved motivation, skill, and commitment. This motivates our focus on causal identification rather than correlational comparison, and underscores the importance of the admissibility and overlap diagnostics reported in Section 5.

5 Results

This section reports effect estimates obtained from causal structures that pass the admissibility gate and evaluates their reliability using effect-level validation. In line with our effect-centric framing, our goal is not to assert the correctness of any single discovered graph,

but to assess whether the target causal effect is identifiable, stable, and robust to falsification under structural uncertainty.

5.1 Target Estimand and Identification

We study users at the individual-user level. Treatment T is defined as any PvP exposure during the first 24 hours after first launch, and outcome Y is Day-1 retention (returning during hours 24–48). The target estimand is:

$$\tau = \mathbb{E}[Y \mid do(T = 1)] - \mathbb{E}[Y \mid do(T = 0)]$$

reported on the risk-difference scale. We adopt backdoor adjustment as the identification strategy. Identification is attempted via backdoor (and generalized) adjustment for each discovered structure after enforcing domain constraints. DoWhy identifies *Web3* as the minimal sufficient adjustment set for graphs that admit identification. All reported main effects condition only on *Web3*. Other variables are retained in the causal graph for structural reasoning but are not included in the adjustment set. In particular, *Total_Session* is not used for adjustment in any reported estimand. Although DoWhy identifies *Web3* as the minimal sufficient adjustment set, this result is not used blindly.

Throughout this work, the target estimand is defined conditional on the analyzed cohort, namely users who became paying players and remained active until the PvP eligibility time t_0 . We do not claim that the estimated effect generalizes to the full player population. Accordingly, all reported effects should be interpreted as cohort-conditional ATEs rather than population-wide causal effects.

Importantly, not all discovered graphs support identification of this estimand. Graphs that fail to admit a valid adjustment set after constraint enforcement yield undefined effects (NaN) and are excluded from effect estimation. We treat such cases as identification failures rather than numerical errors, consistent with the admissibility-first principle of our framework.

5.2 Main Causal Effect

For the subset of graphs that pass the admissibility gate under the specified constraint set, we estimate the effect using multiple estimators. The doubly robust estimator is treated as primary, with regression adjustment and IPW reported for comparison. We obtain:

$$\hat{\tau}_{REG} = 0.155, \quad \hat{\tau}_{IPW} = 0.146, \quad \hat{\tau}_{DR} = 0.143$$

where the DR estimator yields a 95% confidence interval of (0.080, 0.215). This estimate corresponds to one domain-admissible estimand under the imposed temporal and semantic constraints. It indicates that early PvP engagement is associated with an approximately 15% point increase in Day-1 retention among paying players, conditional on the identifying assumptions encoded in the admissible graph.

We emphasize that this effect is not claimed as the unique or true causal effect. Rather, it represents one admissible effect estimate that survives the admissibility gate and serves as a reference point for subsequent stability and falsification analyses.

5.3 Constraint Ladder Ablation For DAG only

We ablate a *constraint ladder* that incrementally injects structural priors, and quantify how these priors change (i) whether the target

Constraint	Identifiable rate (%)	Mean (RD)	ATE	SD (ATE)
C0	0	NaN		NaN
C1	19.05	0.146		0.005
C2	33.33	0.143		0.005
C3	33.33	0.145		0.005

Table 3: Constraint ladder ablation aggregated over all runs (algorithm, α). A run is *identifiable* iff it passes the admissibility gate (valid adjustment set); otherwise ATE is NaN and labeled reject.

ATE is identifiable, (ii) the stability of the estimated effect when identifiable, and (iii) the fraction of runs we should *trust* vs. *reject*.

We consider four constraint levels, from weakest to strongest: **C0** forbids only the edge $R1 \rightarrow other$; **C1** additionally forbids $other \rightarrow Web3$ and keeps $R1 \rightarrow other$ forbidden; **C2** matches the edge prohibitions of **C1** and further forces a semantic edge

($Total_PvE_Battle \rightarrow Total_Session$); **C3** is our full constraint set used elsewhere in the paper. Each level is evaluated across a grid of independence thresholds α and multiple random seeds, and across multiple discovery algorithms. A run is one tuple (algorithm, α).

For each run we compute: (1) Identifiable? a binary gate that is 1 iff an admissible adjustment set exists for the target ATE; otherwise the ATE is treated as undefined. (2) If identifiable, we report the ATE estimate as risk difference (RD). (3) A coarse decision label used for reporting: *trust* if the estimated confidence interval excludes 0 and the ATE is defined; *reject* otherwise.¹

We then aggregate per constraint level:

$$\text{Identifiable Rate} = \frac{1}{N} \sum_{i=1}^N \mathbf{1}\{\widehat{ATE}_i \text{ is defined}\}$$

$$\text{Effect Stability} = \text{SD}\left(\{\widehat{ATE}_i \mid \widehat{ATE}_i \text{ is defined}\}\right)$$

$$\text{Label Rate}_{\text{trust}} = \frac{1}{N} \sum_{i=1}^N \mathbf{1}\{\ell_i = \text{trust}\}$$

Table 3 reports the ablation. Two patterns emerge from the table.

First, tighter domain constraints increase how often the effect is identifiable: the rate moves from 0% (C0) to 19% (C1) and to 33% (C2–C3). Meanwhile, the estimated magnitude changes very little. The difference in mean RD (0.143–0.146) is smaller than the within-setting SD (0.005), indicating that constraints mainly affect identification rather than the value of the estimate.

Second, once identifiable, the results are highly stable. C2 and C3 produce nearly identical means with the same small dispersion. C1 improves identifiability relative to C0, but its variability is not larger than in the tighter regimes.

Finally, C0 yields no identifiable runs. This is compatible with the idea that permissive assumptions admit graphs that block valid adjustment, although the table alone does not determine the mechanism.

¹We did not observe any caution cases in this ablation under our CI rule.

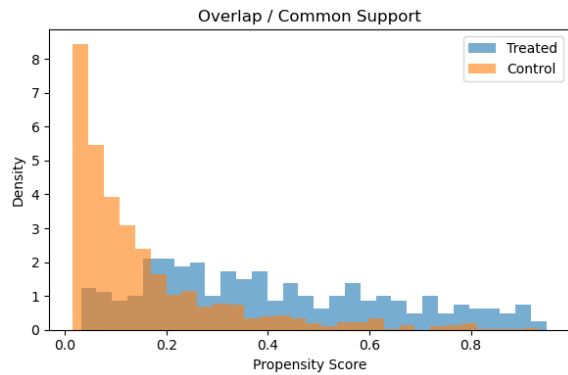


Figure 2: Propensity score distributions for treated (PvP=1) and control (PvP=0) groups. Substantial overlap exists in the common support region [0.032, 0.935].

5.4 Overlap and Positivity Diagnostics

Given the strong self-selection into competitive gameplay evident in Table 2, we conduct detailed overlap diagnostics before proceeding to effect estimation. Backdoor identification requires the positivity assumption, that for all relevant covariate strata, both treated and control users occur with non-zero probability.

Figure 2 displays the propensity score distributions. Treated users exhibit higher propensity scores on average, reflecting self-selection into competitive modes, but the distributions overlap substantially across a wide range. The estimated propensity scores span [0.032, 0.949] for treated users and [0.016, 0.935] for controls, yielding a common support interval of [0.032, 0.935].

We trim observations falling outside common support. Overall, 8.6% of observations are excluded (110 of 1,280 in the analytic sample after initial quality filters), with exclusion concentrated primarily among control users (10.6% of controls vs. 0.8% of treated). This asymmetry reflects that some never-takers, users with covariate profiles making PvP engagement extremely unlikely, have no comparable treated counterparts.

Balance diagnostics confirm that adjustment successfully addresses covariate imbalance. Pre-adjustment standardized mean differences (SMD) are severe: 1.16 for Total_PvE_Battle, 0.92 for Total_Session, and substantial imbalances across other covariates. After inverse probability weighting (IPW), maximum SMD decreases to 0.10, satisfying the conventional $|SMD| \approx 0.1$ threshold for adequate balance.

The effective sample size (ESS) under IPW is 836 out of 1,280 observations, indicating that weighting does not concentrate influence on a small number of units. ESS decomposition shows 116/263 for treated and 735/1017 for controls, confirming adequate representation in both groups.

Taken together, these diagnostics suggest that: (1) sufficient overlap exists to support adjustment-based identification; (2) trimming addresses extreme propensity regions without excessive sample loss; and (3) positivity violations are unlikely to explain the effect patterns observed across discovery algorithms.

5.5 Refutation and Sensitivity Analysis

We subject the domain-admissible effect estimate to three complementary falsification and sensitivity checks designed to probe distinct failure modes: spurious association, sample dependence, and unmeasured confounding.

For placebo treatment, we replace the true treatment with a randomly permuted placebo variable yields an estimated effect statistically indistinguishable from zero ($\approx p = 0.94$). This result indicates that the observed effect is not an artifact of the adjustment procedure or graph structure alone, and does not arise under random assignment of treatment labels.

For data subset stability. We re-estimate the effect on randomly selected data subsets (10%, 50%, 80%, and 90% of the sample). The resulting estimates remain highly consistent (range: 0.142–0.154), with no sign reversal or substantial drift. This suggests that the effect is not driven by a particular subsample or by overfitting to the full dataset.

To assess robustness to unobserved confounding, we conduct a formal sensitivity analysis using E-values on the risk-ratio scale. Using a Poisson regression with robust standard errors and adjusting for the same minimal adjustment set (web3), we estimate the risk ratio of early PvP exposure on Day-1 retention as

$$RR = 1.19 \quad (95\% \text{ CI} : 1.12-1.26).$$

The corresponding E-value for the point estimate is 1.66, and 1.48 for the confidence interval bound closest to the null. This implies that an unmeasured confounder would need to be associated with both PvP participation and retention by a risk ratio of at least 1.66 each, above and beyond the measured covariates, to fully explain away the observed effect. Restricting the analysis to paying users who remain active until t_0 may introduce selection effects if latent traits jointly influence cohort membership, treatment adoption, and retention. While such selection-induced confounding cannot be ruled out, the E-value analysis quantifies the minimum strength such unobserved factors would need to fully explain away the observed effect. Moreover, several major drivers of selection (e.g., early engagement intensity and platform commitment) are partially observed and adjusted for, which likely attenuates, but does not eliminate this risk. We emphasize that the E-value is used here as a diagnostic rather than a pass/fail criterion. In telemetry settings with strong self-selection and feedback, no single robustness metric is decisive; instead, E-values should be interpreted jointly with identifiability, stability across admissible structures, and falsification tests.

Taken together, these refutation and sensitivity analyses do not eliminate all possible sources of bias, but they fail to falsify the domain-admissible effect under three distinct diagnostics: randomized treatment assignment, subsample perturbation, and bounded unmeasured confounding. We therefore interpret the estimated effect as moderately robust under the assumptions encoded by the admissibility gate, while emphasizing that it remains conditional on the absence of strong unmeasured confounders.

5.6 Effect Behavior under Minimally Constrained Discovery

We examine effect estimates obtained from discovery using only minimal temporal constraints (e.g., forbidding future-to-past and outcome-to-covariate edges), without enforcing domain-semantic or measurement constraints.

Under this setting, PC identifies a valid estimand for only 3 out of 7 significance thresholds ($\alpha \in \{0.001, 0.005, 0.01\}$), yielding nearly identical effects around $\hat{\tau} \approx 0.155$.

For larger thresholds ($\alpha \geq 0.02$), the learned structures fail the admissibility gate and effect estimation becomes undefined (NaN), due to unresolved adjacencies that violate backdoor identifiability.

Notably, even when the direct edge from PvP exposure to retention is absent, the effect remains identifiable through indirect causal pathways, leading to the same total effect estimate.

These results show that minimal temporal constraints alone are insufficient to guarantee causal identifiability. Graphs that are statistically compatible with conditional independence tests may still fail to support effect estimation once weak causal ordering requirements are enforced.

5.7 Effect Stability Across Discovery Algorithms

We compare discovery algorithms by (i) admissibility under domain constraints and (ii) stability of the estimated ATE across $\alpha \in \{0.001, \dots, 0.2\}$.

Using DAG, only a subset of methods consistently pass the admissibility gate. Score-based BOSS is admissible for all thresholds and yields an estimate across the grid ($\hat{\tau} = 0.144$, variance ≈ 0). PC, GRaSP are admissible for several thresholds and produce highly stable effects around $\hat{\tau} \approx 0.143$ when identification is possible.

A subset of PAG-based discovery runs admit point-identified causal queries across all tested levels. Empirically, PC is the only method that consistently delivers identifiable effects, with CFCI doing so in just one case. Most other FCI-type approaches return non-identifiable results. Therefore, claims about convergence, dispersion, or attenuation of their estimates are largely inapplicable; the primary issue is the absence of identification rather than differences in numerical values. These results are reported separately to distinguish identification under partial orientation from the fully directed DAG-based analysis.

Overall, effect stability is algorithm-dependent and conditional on admissibility. Latent awareness or graph-level fit alone does not imply that a target causal query is identifiable or yields a reliable effect estimate.

5.8 Summary of Findings

Our results show that causal identifiability, rather than graph accuracy, is the primary bottleneck in telemetry-driven discovery. Many statistically admissible graphs do not support effect estimation under our admissibility criterion once minimal temporal and semantic constraints are enforced, with this behavior occurring most frequently for outputs of latent-aware methods such as FCI and GRaSP-FCI.

When identification is possible, several algorithm families (PC, GRaSP, BOSS) converge to a stable effect magnitude around $\hat{\tau} \approx$

0.144, despite producing different graph structures. This convergence occurs even when direct causal edges are absent, as the effect is preserved through indirect causal pathways.

These findings support an effect-centric evaluation paradigm focused on admissibility and stability rather than structural recovery metrics. Reliability cannot be inferred from graph-level properties or algorithm labels alone, but must be established through effect-level validation under structural uncertainty.

6 Conclusion

We proposed an admissibility-first, effect-centric framework for evaluating causal discovery in telemetry-driven systems with feedback and self-selection. Using real game telemetry, we show that many statistically admissible graphs do not yield estimable causal effects under our admissibility criterion once minimal temporal and semantic constraints are enforced, particularly for outputs of latent-aware methods such as FCI and GRaSP-FCI.

When identification is possible, several algorithm families (PC, GRaSP, BOSS) converge to a stable effect despite producing structurally different graphs. This demonstrates that structural agreement is not required for effect-level stability and highlights the role of indirect causal pathways in preserving total effects.

We do not claim the reported effect is immune to all forms of unmeasured confounding or selection. Rather, the contribution of this work is to demonstrate how an admissibility-first, effect-centric workflow can identify effects that are decision-consistent and stable under structural uncertainty.

Overall, our results indicate that latent-awareness or graph recovery accuracy alone does not guarantee identifiability or reliability of a target causal query. Reliable causal inference in feedback-driven telemetry data requires prioritizing admissibility, stability, and falsification of effects over graph-level metrics. This work provides a practical pathway for using causal discovery to support decision-making in interactive systems. From a decision-support perspective, identifying whether an effect is admissible and stable under realistic structural uncertainty is often more actionable than pursuing maximal theoretical identification.

References

- [1] Bryan Andrews, Joseph Ramsey, and Gregory F Cooper. 2019. Learning high-dimensional directed acyclic graphs with mixed data-types. In *The 2019 ACM SIGKDD Workshop on Causal Discovery*. PMLR, 4–21.
- [2] Bryan Andrews, Joseph Ramsey, Ruben Sanchez Romero, Jazmin Camchong, and Erich Kummerfeld. 2023. Fast scalable and accurate discovery of dags using the best order score search and grow shrink trees. *Advances in neural information processing systems* 36 (2023), 63945–63956.
- [3] Trambak Banerjee, Gourab Mukherjee, Shantanu Dutta, and Pulak Ghosh. 2020. A large-scale constrained joint modeling approach for predicting user activity, engagement, and churn with application to freemium mobile games. *J. Amer. Statist. Assoc.* (2020).
- [4] Patrick Blöbaum, Peter Götz, Kailash Budhathoki, Atalanti A. Mastakouri, and Dominik Janzing. 2024. DoWhy-GCM: An Extension of DoWhy for Causal Inference in Graphical Causal Models. *Journal of Machine Learning Research* 25, 147 (2024), 1–7. <http://jmlr.org/papers/v25/22-1258.html>
- [5] Sarthak Chakraborty, Shaddy Garg, Shubham Agarwal, Ayush Chauhan, and Shiv Kumar Saini. 2023. Causil: Causal graph for instance level microservice data. In *Proceedings of the ACM Web Conference 2023*. 2905–2915.
- [6] Anders Harboell Christiansen, Emil Gensby, and Bryan S Weber. 2019. Resolving simultaneity bias: using features to estimate causal effects in competitive games. In *2019 IEEE Conference on Games (CoG)*. IEEE, 1–8.
- [7] Shaobo Cui, Luca Mouchel, and Boi Faltings. 2025. Uncertainty in Causality: A New Frontier. In *Proceedings of the 63rd Annual Meeting of the Association for Computational Linguistics (Volume 1: Long Papers)*. 8022–8044.

- [8] Philipp M Faller, Leena C Vankadara, Atalanti A Mastakouri, Francesco Locatello, and Dominik Janzing. 2024. Self-compatibility: Evaluating causal discovery without ground truth. In *International Conference on Artificial Intelligence and Statistics*. PMLR, 4132–4140.
- [9] Chen Gao, Yu Zheng, Wenjie Wang, Fuli Feng, Xiangnan He, and Yong Li. 2024. Causal inference in recommender systems: A survey and future directions. *ACM Transactions on Information Systems* 42, 4 (2024), 1–32.
- [10] Amanda Gentzel, Dan Garant, and David Jensen. 2019. The case for evaluating causal models using interventional measures and empirical data. *Advances in Neural Information Processing Systems* 32 (2019).
- [11] Azam Ikram, Sarthak Chakraborty, Subrata Mitra, Shiv Saini, Saurabh Bagchi, and Murat Kocaoglu. 2022. Root cause analysis of failures in microservices through causal discovery. *Advances in Neural Information Processing Systems* 35 (2022), 31158–31170.
- [12] Amin Jaber, Adele Ribeiro, Jiji Zhang, and Elias Bareinboim. 2022. Causal identification under Markov equivalence: calculus, algorithm, and completeness. *Advances in Neural Information Processing Systems* 35 (2022), 3679–3690.
- [13] Hyunjae Kang, Changwoo Suh, and Huy Kang Kim. 2024. Match experiences affect interest: Impacts of matchmaking and performance on churn in a competitive game. *Heliyon* 10, 3 (2024).
- [14] Bikram Karmakar, Peng Liu, Gourab Mukherjee, Hai Che, and Shantanu Dutta. 2022. Improved retention analysis in freemium role-playing games by jointly modelling players’ motivation, progression and churn. *Journal of the Royal Statistical Society Series A: Statistics in Society* 185, 1 (2022), 102–133.
- [15] Jongho Kim, Kihan Kim, Hansol Kim, and Shanshan Li. 2026. Analyzing player churn in esports games: a survival analysis of league of legends log data. *Sport, Business and Management: An International Journal* (2026), 1–22.
- [16] Wai-Yin Lam, Bryan Andrews, and Joseph Ramsey. 2022. Greedy relaxations of the sparsest permutation algorithm. In *Uncertainty in Artificial Intelligence*. PMLR, 1052–1062.
- [17] Mingxuan Liu, Jack Lipei Tang, and Dmitri Williams. 2025. Sympathy for the devil: Serial mediation models for toxicity, community, and retention. *Media and Communication* 13 (2025).
- [18] Juan Miguel Ogarrio, Peter Spirtes, and Joe Ramsey. 2016. A hybrid causal search algorithm for latent variable models. In *Conference on probabilistic graphical models*. PMLR, 368–379.
- [19] Kunwoo Park, Meeyoung Cha, Haewoon Kwak, and Kuan-Ta Chen. 2017. Achievement and friends: Key factors of player retention vary across player levels in online multiplayer games. In *Proceedings of the 26th international conference on world wide web companion*. 445–453.
- [20] Luan Pham, Huang Ha, and Hongyu Zhang. 2024. Root cause analysis for microservice system based on causal inference: How far are we?. In *Proceedings of the 39th IEEE/ACM International Conference on Automated Software Engineering*. 706–715.
- [21] Vineet K Raghu, Allen Poon, and Panayiotis V Benos. 2018. Evaluation of causal structure learning methods on mixed data types. In *Proceedings of 2018 ACM SIGKDD Workshop on Causal Discovery*. PMLR, 48–65.
- [22] Vineet K Raghu, Joseph D Ramsey, Alison Morris, Dimitrios V Manatakis, Peter Sprites, Panos K Chrysanthis, Clark Glymour, and Panayiotis V Benos. 2018. Comparison of strategies for scalable causal discovery of latent variable models from mixed data. *International journal of data science and analytics* 6, 1 (2018), 33–45.
- [23] Joseph Ramsey, Bryan Andrews, and Peter Spirtes. 2025. Efficient Latent Variable Causal Discovery: Combining Score Search and Targeted Testing. *arXiv preprint arXiv:2510.04263* (2025).
- [24] Joseph Ramsey, Jiji Zhang, and Peter L Spirtes. 2012. Adjacency-faithfulness and conservative causal inference. *arXiv preprint arXiv:1206.6843* (2012).
- [25] Amit Sharma and Emre Kiciman. 2020. DoWhy: An End-to-End Library for Causal Inference. *arXiv preprint arXiv:2011.04216* (2020).
- [26] Peter Spirtes, Clark N Glymour, and Richard Scheines. 2000. *Causation, prediction, and search*. MIT press.
- [27] Tyler J VanderWeele and Peng Ding. 2017. Sensitivity analysis in observational research: introducing the E-value. *Annals of internal medicine* 167, 4 (2017), 268–274.
- [28] Shuyuan Xu, Jianchao Ji, Yunqi Li, Yingqiang Ge, Juntao Tan, and Yongfeng Zhang. 2025. Causal Inference for Recommendation: Foundations, Methods, and Applications. *ACM Transactions on Intelligent Systems and Technology* 16, 3 (2025), 1–51.
- [29] Hao Zhou, Rongxiao Huang, Shaoming Li, Guibin Jiang, Jiaqi Zheng, Bing Cheng, and Wei Lin. 2024. Decision focused causal learning for direct counterfactual marketing optimization. In *Proceedings of the 30th ACM SIGKDD Conference on Knowledge Discovery and Data Mining*. 6368–6379.

A Algorithm Details

We evaluate 10 causal discovery algorithms grouped by inference mechanism:

Constraint-based: PC, FCI [26], FCFCI [24], and FCI-MAX [22] use conditional independence (CI) tests to prune edges. They employ the Degenerate Gaussian Likelihood Ratio Test [1] to handle mixed data.

Score-based: BOSS [2] and GRaSP [16] explore permutation space and maximize Degenerate Gaussian BIC scores.

Hybrid: GFCCI [18], BOSS-FCI, and GRaSP-FCI [23] combine score-based search with FCI-style refinement.

Metric	PC	GFCCI	FCI	BOSS	BOSS-FCI	GRASP-FCI	GRASP	FCI-MAX	FCFI
precision	0.17	0.33	0.19	0.04	0.24	0.27	0.06	0.16	0.33
recall	0.22	0.56	0.33	0.11	0.44	0.44	0.22	0.33	0.44
tp	2.00	5.00	3.00	1.00	4.00	4.00	2.00	3.00	4.00
fp	10.00	10.00	13.00	24.00	13.00	11.00	32.00	16.00	8.00
fn	7.00	4.00	6.00	8.00	5.00	5.00	7.00	6.00	5.00
adj_precision	0.38	0.45	0.42	0.24	0.42	0.45	0.19	0.38	0.45
adj_recall	0.56	0.56	0.56	0.89	0.56	0.56	0.78	0.56	0.56
adj_tp	5.00	5.00	5.00	8.00	5.00	5.00	7.00	5.00	5.00
adj_fp	8.00	6.00	7.00	25.00	7.00	6.00	29.00	8.00	6.00
adj_fn	4.00	4.00	4.00	1.00	4.00	4.00	2.00	4.00	4.00
shd	15.00	14.00	15.00	33.00	15.00	13.00	36.00	16.00	11.00

Table 4: Graph deviation metrics relative to domain-consistent baseline

B Edge Constraints Specification

Table 5: Domain Constraints and Rationale

Constraint	Edge	Rationale
Temporal	R1 \rightarrow * (forbidden)	Outcomes cannot cause prior behaviors
Platform-level	* \rightarrow Web3 (forbidden)	Wallet is system prerequisite, not gameplay outcome
Measurement	PvE \rightarrow Total_Session	Total_Session is composite aggregate
Semantic	PvP \nrightarrow onboarding	Combat doesn’t cause onboarding friction

All constraints are pre-specified based on telemetry construction and system design, applied prior to discovery, and do not encode assumptions about effect magnitude or sign.

C Model Validation Details

C.1 Functional Causal Model Assumptions

We assess FCM assumptions using independence tests between noise terms and parents. Across all mechanisms (LogReg, Decision Tree, HistGradientBoosting), p-values exceed 0.70 for Total_Session and equal 1.0 for Time_Play_Level1 and Total_PvE_Battle, indicating no evidence against assumed causal mechanisms.

C.2 Calibration Metrics

Logistic Regression achieves lowest CRPS for the retention outcome (0.159), indicating superior calibration.

Table 6: CRPS by Node and Mechanism

Node	LogReg	DT	HistGB	Assessment
R1	0.159	0.215	0.184	Very Good
PvP	0.166	0.167	0.168	Very Good
Time_Play_Level1	0.503	0.502	0.499	Fair
Total_PvE_Battle	0.467	0.528	0.473	Fair
Total_Session	0.478	0.475	0.479	Fair

C.3 Intrinsic Causal Contribution

Table 7: ICC Values by Mechanism

Mechanism	ICC (%)
Logistic Regression	63
Decision Tree	38
HistGradientBoosting	60

Over 63% of retention variance is explained by the modeled causal structure under Logistic Regression.

D Positivity Diagnostics

Table 8: Overlap and Balance Diagnostics

Metric	Before Trim	After Trim
<i>Sample Size</i>		
Total N	1,280	1,170
Treated	263	261
Control	1,017	909
<i>Propensity Score Range</i>		
Treated	[0.032, 0.949]	[0.032, 0.910]
Control	[0.016, 0.935]	[0.032, 0.935]
Common support	[0.032, 0.935]	[0.032, 0.910]
<i>Effective Sample Size (IPW)</i>		
Overall	836.0	741.6
Treated	116.2	115.8
Control	734.7	647.3
<i>Covariate Balance (SMD post-IPW)</i>		
Total_PvE_Battle	0.093	0.004
Total_Session	0.102	0.023
Web3	0.012	0.104
Time_Play_Level1	0.008	0.011
Max SMD	0.102	0.104

E Effect-Centric Validation Protocol

Inputs: Observational telemetry with temporal slicing; minimal domain constraints.

Step 1 – Data Preparation: Define unit of analysis and temporal windows; enforce temporal precedence; distinguish primitive from composite variables.

Step 2 – Causal Discovery: Apply multiple algorithms under domain constraints; allow multiple admissible structures.

Step 3 – Admissibility Gate: Proceed only with graphs satisfying: acyclicity, constraint compliance, valid identification strategy, adequate positivity.

Step 4 – Effect Estimation: Estimate target effect under each admissible graph; record magnitude and uncertainty.

Step 5 – Stability Analysis: Compare effects across algorithms; assess sensitivity to α thresholds; identify invariant vs. sensitive estimates.

Step 6 – Falsification: Placebo intervention; data subsampling tests.

Decision:

- Trust: Effect stable and falsification passed
- Caution: Sign-consistent but magnitude sensitive
- Reject: Effect unstable or falsified

F Exploratory PAG-based Point Estimates

Method family	Typical output	Used in main stability claims
(some) PC / BOSS / GRaSP	DAG	Yes
(some) PC/ (some) CFCI	PAG	No

Table 9: Summary of Causal Discovery Method Families

Method	Mean ATE	SD	Identifiable runs (α)
PC	0.144	0.000	4
FCI	0.194	0.000	7
GFCI	0.194	0.000	7
BOSS-FCI	0.138	0.047	7
GRaSP-FCI	0.138	0.047	7
FCI-MAX	0.187	0.018	7
CFCI	0.151	0.064	7

Table 10: Effect estimates from identifiable PAG-based discovery runs across different significance levels